



Long-Term Cultures of Spinal Cord Interneurons

Ingrid Vargova^{1,2}, Jan Kriska³, Jessica C. F. Kwok^{4,5}, James W. Fawcett^{4,6} and Pavla Jendelova^{1,2*}

¹ Department of Neuroregeneration, Institute of Experimental Medicine, Czech Academy of Sciences, Prague, Czechia, ² Second Faculty of Medicine, Charles University, Prague, Czechia, ³ Department of Cellular Neurophysiology, Institute of Experimental Medicine, Czech Academy of Sciences, Prague, Czechia, ⁴ The Center for Reconstructive Neurosciences, Institute of Experimental Medicine, Czech Academy of Sciences, Prague, Czechia, ⁵ Faculty of Biological Sciences, University of Leeds, Leeds, United Kingdom, ⁶ John van Geest Centre for Brain Repair, Department of Clinical Neurosciences, University of Cambridge, Cambridge, United Kingdom

Spinal cord interneurons (SpINs) are highly diverse population of neurons that play a significant role in circuit reorganization and spontaneous recovery after spinal cord injury. Regeneration of SpIN axons across rodent spinal injuries has been demonstrated after modification of the environment and neurotrophin treatment, but development of methods to enhance the intrinsic regenerative ability of SpINs is needed. There is a lack of described *in vitro* models of spinal cord neurons in which to develop new regeneration treatments. For this reason, we developed a new model of mouse primary spinal cord neuronal culture in which to analyze maturation, morphology, physiology, connectivity and regeneration of identified interneurons. Isolated from E14 mice, the neurons mature over 15 days *in vitro*, demonstrated by expression of maturity markers, electrophysiological patch-clamp recordings, and formation of synapses. The neurons express markers of SpINs, including Tlx3, Lmx1b, Lbx1, Chx10, and Pax2. The neurons demonstrate distinct morphologies and some form perineuronal nets in long-term cultivation. Live neurons in various maturation stages were axotomized, using a 900 nm multiphoton laser and their fate was observed overnight. The percentage of axons that regenerated declined with neuronal maturity. This model of SpINs will be a valuable tool in future regenerative, developmental, and functional studies alongside existing models using cortical or hippocampal neurons.

Keywords: spinal interneurons, culture, maturation, axon regeneration, laser axotomy

OPEN ACCESS

Edited by:

Daniela Tropea,
Trinity College Dublin, Ireland

Reviewed by:

Kai Liu,
Hong Kong University of Science
and Technology, Hong Kong SAR,
China
Kirsten Haastert-Talini,
Hannover Medical School, Germany

*Correspondence:

Pavla Jendelova
pavla.jendelova@iem.cas.cz

Specialty section:

This article was submitted to
Cellular Neurophysiology,
a section of the journal
Frontiers in Cellular Neuroscience

Received: 02 December 2021

Accepted: 12 January 2022

Published: 07 February 2022

Citation:

Vargova I, Kriska J, Kwok JCF,
Fawcett JW and Jendelova P (2022)
Long-Term Cultures of Spinal Cord
Interneurons.
Front. Cell. Neurosci. 16:827628.
doi: 10.3389/fncel.2022.827628

INTRODUCTION

The intrinsic regeneration capacity of mature mammalian central nervous system (CNS) is poor. This makes spinal cord injury (SCI) a detrimental condition that represents one of the major causes of disability, and treatment possibilities are limited. However, continued research in the field has led to an increased understanding of the causes of the regeneration failure, which if appropriately modulated, can be used for treatment of the SCI. The extracellular environment of the CNS is not favorable for axon outgrowth due to production of growth-inhibiting molecules such as NogoA and CSPGs from glial scars surrounding the damaged tissue (Shen et al., 2009; Schwab and Strittmatter, 2014; Uyeda and Muramatsu, 2020), and there is a lack of some necessary growth factors that provide trophic support for neurons and act as chemoattractants for axons (Blesch et al., 2012; Anderson et al., 2018). Another important limiting factor is the intrinsic loss of regenerative ability

in CNS neurons that comes with neuronal maturation. Various factors contribute to this loss of regeneration, including failure of CNS neurons to activate appropriate transcriptional, translational and epigenetic programs at appropriate subcellular locations that would enable axon growth after injury (van Niekerk et al., 2016; Petrova et al., 2021), changes in axonal transport that exclude growth-related molecules from mature axons and decreased signaling in some pathways. A high level of intrinsic regeneration ability is present in immature neurons but ceases abruptly with maturation (Nicholls and Saunders, 1996; Lu et al., 2014; Koseki et al., 2017).

Maturation and aging in the CNS involve complex and numerous pathways, so it is challenging to study their effect on the regeneration ability of neurons *in vivo*. *In vitro* models, on the other hand, can offer a wide variety of tools to study individual neuronal cell types, to regulate and describe neuronal behavior, and to uncover molecular pathways relating to development and regeneration of neurons (Abu-Rub et al., 2010; Franssen et al., 2015). Therefore, describing axon growth inhibition mechanisms *in vitro* is a valuable approach that could lead to further comprehension of the limits of CNS regeneration and subsequently to discovery of new therapeutic avenues. Various *in vitro* models have been established to explore CNS axon regeneration. These include primary cell cultures created by dissociating neural tissue from animals at various ages (Donaldson and Höke, 2014). Dorsal root ganglia (DRGs) (Cheah et al., 2016), hippocampal (Kaech and Banker, 2006; Moore et al., 2009), and cortical cultures (Koseki et al., 2017) are among the most commonly used models. Primary spinal cord cultures have been described as well (Thomson et al., 2008; Eldeiry et al., 2017), but their application in axon regeneration studies has so far been limited. Investigation of the regenerative capacity of spinal interneurons (SpINs) is of particular interest, as it was shown, that less severe, anatomically incomplete SCI can result in partial recovery that follows after spontaneous reorganization of neural circuits (Bareyre et al., 2004; Martinez et al., 2012), and growth of spinal interneuron neurites across mouse spinal injuries can be stimulated by treatments to enhance neuronal regenerative ability, astrocyte permissiveness and axonal chemoattraction (Anderson et al., 2016). Key components of neuroplasticity in these incomplete lesions are SpINs, as they form alternative routes to convey information between cells above and below the lesion (Courtine et al., 2008; May et al., 2017).

Here, we describe a robust model of long-term dissociated embryonic spinal cord cultures. During cultivation, neurons in these cultures form synapses, acquire mature electrical properties and markers of mature neurons, lose regenerative capacity, and express markers of SpINs. The culture model will be valuable for future developmental, functional as well as axonal regeneration studies.

MATERIALS AND METHODS

Cell Culture

The method of generating mature spinal cord neurons was based on previously published methods for culturing spinal

cord (Thomson et al., 2008), hippocampal and cortical neurons (Barbati et al., 2013; Koseki et al., 2017; Petrova et al., 2020), with modifications. Spinal neurons were isolated from E13.5-E14.5 embryos of the C57BL/6J mice. Spinal cords were dissected from embryos immersed in a cold Hibernate-E medium (Gibco, Thermo Fisher). The meninges were removed, and tissue was stored over ice in Hibernate-E (Gibco, Thermo Fisher). The collected tissue was washed with 1 ml of HBSS without Ca^{2+} or Mg^{2+} (Gibco, Thermo Fisher) two times. Next, the tissue was digested in papain-based Neuron Isolation Enzyme (Thermo Scientific™ Pierce) by adding 30 μl of enzyme solution per 1 spinal cord for 9 min at 37°C. After digestion, the enzyme was carefully removed, and the tissue was placed in disruption medium 1 (DM1) (Table 1). Tissue was disrupted by trituration with P1000 tip and left to settle for 2 min. The supernatant was transferred to a new tube, while the tissue pellet was triturated again in disruption medium 2 (DM2) (Table 1). This step was repeated once more if any tissue fragments remained after the second disruption. Supernatant containing disrupted tissue was transferred by a polished Pasteur pipette into a new falcon tube through a 40 μm cell strainer to remove undisrupted tissue fragments. Plating medium (PM) (Table 1) was added in a 1:1 ratio to the filtered solution containing the cells. The cell suspension was centrifuged for 5 min at 90 g at 37°C, the supernatant was removed, and the pellet was resuspended in 2 ml of PM. Then, the cells were counted (approximate expected amount is 1.2 million cells per spinal cord) and plated on glass coated with 100 $\mu\text{g}/\text{ml}$ poly-D-lysine (Thermo Fisher) dissolved in pH 8.6 borate buffer. The cells were cultured either in a 24-well plate on sterilized 12 mm borosilicate glass coverslips (Karl Hecht), or glass-bottom 10-well CELLview™ Cell Culture Slides (Greiner). The optimal plating density of dissociated spinal cord cells in our cultures was around 93,000 cells/cm². The best plating method that resulted in evenly distributed cells on the coverslips, was to dilute the dissociated cells in PM to a final concentration of 500,000 cells/ml and then add 350 μl of cell suspension into 24-well plate, or 80 μl into 10-well cell culture slide. After 1 h, most of the cells adhered to the coverslips, and cultivation medium (CM) was added to the PM in 1:1 proportion, but not before some of the PM was discarded. Final media volume used for cultivation in the 24-well plate was 500 μl and in the 10-well cell culture slide, it was 150 μl . Cultures were maintained by exchanging 1/2 of the media volume every 2 days. To limit the proliferation of glia, CM with the ITS+ supplement was replaced with CM without ITS+ after 7 days of culture. Importantly, we were able to maintain the cultures for 72 days.

Plasmid Transfection

Cultures were transfected with CAG-GFP plasmid using NeuroMag magnetofection (OZ Biosciences) at DIV3. The CM was removed from the wells, stored, and replaced with 80% of regular cultivation volume of unsupplemented MACS Neuro Medium (Miltenyi Biotech). An appropriate amount of DNA plasmid was mixed with magnetic beads in OptiMEM medium (Gibco, Thermo Fisher) and incubated for 15 min at room temperature (RT), facilitating the binding reaction. The amount of reagents used for the transfection depended on the

TABLE 1 | Media compositions used for preparation and maintaining spinal cord cultures.

Medium	Composition	Approximate total volume needed
Disruption medium 1 (DM1)	Hibernate-E (Gibco, Thermo Fisher), 0.8% BSA (Sigma-Aldrich) 100 µg/ml DNase (Sigma-Aldrich)	1 ml
Disruption medium 2 (DM2)	Hibernate-E, 0.4% BSA 20 µg/ml DNase	2 ml
Plating medium (PM)	50% DMEM, low glucose (Gibco, Thermo Fisher) 25% Horse serum (Gibco, Thermo Fisher) 25% HBSS without Ca ²⁺ or Mg ²⁺ (Gibco, Thermo Fisher) 1% Penicillin-Streptomycin (10,000 U/mL) (Gibco, Thermo Fisher)	30 ml
Cultivation medium (CM)	MACS Neuro Medium (Miltenyi Biotec) 2% NeuroBrew 21 (Miltenyi Biotec) 1% Glutamax (Thermo Fisher) *1% ITS+ (Sigma-Aldrich) 1% Penicillin-Streptomycin	50 ml

*ITS+ was excluded from cultivation media in cultures cultivated for more than 7 days.

cultivation volume of the particular plate used in experiment. The proportions were calculated according to an optimized 24-well plate protocol, where 0.2 µg of DNA, 0.8 µl of magnetic beads, and 100 µl of OptiMEM were added per well. OptiMEM volume represented 20% of the regular cultivation volume. After the incubation, the mixture was added dropwise into wells with cells and unsupplemented medium. Plates were incubated on top of a strong magnet, purchased along with NeuroMag Starting Kit (OZ Biosciences), for 20 min at 37°C. The magnetic plate was removed and cells were incubated for another 40 min, after which original CM was returned to the wells. GFP was expressed in the culture 24 h after transfection. The conditions of transfection were optimized to attain low-efficacy transfection so that only a few of the cells in the culture expressed GFP and their morphology could be observed.

Immunocytochemistry

Cells were fixed using 4% paraformaldehyde in phosphate-buffered saline (PBS) for 15 min at RT, washed twice, and kept in PBS at 4°C until further use. The staining protocol was started with permeabilization and blocking of the sample using solution containing 10% goat or donkey serum (according to secondary antibodies used) and 0.4% Triton-X in PBS for 1 h at RT with shaking. Next, primary antibodies were diluted in 2% goat serum and 0.1% Triton-X in PBS according to concentrations indicated in **Table 2**. Primary antibodies were incubated with the cells overnight at 4°C with gentle shaking, after which the solution was aspirated and the coverslips were washed twice with PBS. Secondary antibodies, diluted in the same solution as primary antibodies, were incubated with the samples for 1 h at RT. Next, nuclei were stained with DAPI (1/3,000 in PBS) for 5 min.

Coverslips were then washed two times with PBS and mounted on microscopy slides with Aqua-Poly/Mount (Polysciences) and kept in the dark at 4°C until imaging.

Microscopy and Image Analysis

Brightfield images of live cultures were captured on a Zeiss Axio Vert.A1 inverted microscope equipped with AxioCam ERC 5s camera.

Fluorescence microscopy of the cultures was done on a LEICA CTR 6500 microscope. Analysis of neuronal and non-neuronal composition of the culture during cultivation was done by counting DAPI+ nuclei and DAPI+ nuclei colocalized with βIII-tubulin-positive cells with Fiji software (Schindelin et al., 2012). Expression of doublecortin (DBC) and neurofilament 70 kDa (NF70) during cultivation was analyzed by measuring the average gray value of captured fluorophore of a random region on coverslips using Fiji software. To define the background signal, the mean gray value was also measured in three random, smaller areas of the analyzed region without apparent signal. Morphological analysis of GFP-transfected neurons was performed using Fiji SNT plugin (Arshadi et al., 2020). Analyzed morphological metrics were: average length of branches, cable length, number of branches, axonal length, number of axonal branch points, length of axonal branches, average dendrite length, cable length of dendrites, and number of dendrites. Axons and dendrites were identified by morphologic norms established by Kaech and Banker (2006).

Confocal microscopy images were captured on a Zeiss LSM 880 Airyscan inverted microscope. Confocal images were used for presynaptic and postsynaptic marker colocalization analysis as well as spinal cord neuronal markers visualization. A Z-stack of images with 0.5 µm thickness increment was captured in random regions of the coverslip. Maximum frontal orthogonal projection of the Z-stack made in ZEN 3.1 (blue edition) was used for colocalization analysis. Synapses were counted using Puncta Analyzer v2.0, a Fiji plugin written by Bary Wark¹.

Laser Axotomy

Cells cultured on Greiner Bio-One CELLview™ Cell Culture Slides, transfected with GFP plasmid at DIV3, were kept in the microscope incubation chamber at 37°C and 5% CO₂. After finding regions of interest, cells were captured before cutting using Carl Zeiss AxioObserver.Z1 microscope with confocal module LSM 880 NLO. Objective LD LCI Plan-Apochromat 25x/0.8 Imm Corr DIC M27 with oil immersion was used in the experiment. Next, axotomy was performed using a Ti: Sapphire femtosecond laser Chameleon Ultra II (Coherent), set at 900 nm. The cut was achieved by scanning a 3.4 µm long line across the axon, approximately 250 µm (253.8 ± 75.160 µm) from the cell body, in line-scan mode repeatedly 100–200 times, using 80–100% of the laser power. Axons were identified by morphologic norms established by Kaech and Banker (2006). Cells were then scanned every 30 min for 14 h to observe the post-axotomy response. Images were analyzed using ZEN 3.1 (blue edition) (Carl Zeiss Microscopy GmbH) and Fiji.

¹<https://github.com/physion/puncta-analyzer>

Electrophysiological Recordings

The patch-clamp technique in the whole-cell configuration was used to evaluate the cell membrane properties of neurons. Micropipettes with a tip resistance of approximately 10 M Ω were made of borosilicate glass using a P-97 Flaming/Brown micropipette puller (Sutter Instruments) and filled with intracellular solution (0.5 mM CaCl₂, 130 mM KCl, 2 mM MgCl₂, 3 mM ATP, 5 mM EGTA, and 10 mM HEPES with pH 7.2). Coverslips with the cultures were placed on the recording chamber of an upright Axioskop microscope (Zeiss), equipped with a high-resolution AxioCam HR digital camera (Zeiss) and electronic micromanipulators (Luigs and Neumann). Electrophysiological data were recorded on cells perfused in artificial cerebrospinal fluid (2.7 mM KCl, 135 mM NaCl, 1 mM MgCl₂, 2.5 mM CaCl₂, 10 mM glucose, 1 mM Na₂HPO₄ and 10 mM HEPES with osmolality 312.5 \pm 2.5 mOsmol/kg and pH 7.4). The signals were measured with a 10 kHz sample frequency and amplified with an EPC9 amplifier, controlled by the PatchMaster software (HEKA Elektronik), and filtered using a Bessel filter. Resting membrane potential (E_m) was recorded by switching the EPC9 amplifier to the current-clamp mode. Raw data were processed with the FitMaster software (HEKA Elektronik). Input resistance (IR) was assessed from the current value at 40 ms after the onset of the 50 ms depolarizing pulse from the holding potential of -70 mV to -60 mV. Membrane capacitance (C_m) was determined by Lock-in protocol in the PatchMaster software. To measure the sodium currents (I_{Na+}), neurons were depolarized, and amplitude of the current was recorded at voltage step with the maximal current activation. In order to isolate the Na⁺ component only, the time- and voltage-independent currents were subtracted, and the peak value was considered the I_{Na+} . Action potentials (AP) were recorded in the current-clamp mode. The current varied from 50 pA to 1 nA, in 50 pA increments; the pulse duration was 300 ms. Cells that produced at least one AP were considered capable of generating AP.

Statistics

Statistically significant differences between multiple time points during culture cultivation groups were determined by Mann-Whitney test, one-way or two-way ANOVA, followed by Tukey's multiple comparisons *post hoc* test (GraphPad Prism 9 software). Differences were regarded as significant at $p < 0.05$. Graphs were drawn using GraphPad Prism 9 software as means \pm standard error of the mean (SEM), while the level of statistical significance was marked as follows: * $p < 0.05$, ** $p < 0.01$, *** $p < 0.001$.

RESULTS

The study aimed to establish culture conditions that would enable stable cultivation, maturation, and characterization of spinal cord interneurons isolated from E14 mice embryos. The composition of the culture during cultivation was analyzed using immunocytochemistry; maturity of the neurons was analyzed by immunocytochemistry and patch-clamp, and regenerative capacity of neurons was established by laser axotomy.

Cellular Composition Changes During Cultivation

At day *in vitro* (DIV) 1, cells were attached and started to grow processes (Figure 1). Cells formed processes at DIV1, which extended during DIV3 and DIV10. Formation of complex network of processes over the whole culture surface could be seen at DIV17, and more robustly in older cultures at DIV41 and DIV70.

The total number of neurons in spinal cord culture was assessed by counting β III-tubulin-positive cells per unit area of the fluorescence microscopy images (Figure 2). Although the total number of neurons remained stable (Figure 2E), the total number of cells, assessed by counting DAPI-stained nuclei in the culture, continued to rise during cultivation (Figure 2F). Due to the proliferation of glia, the neuronal fraction of the culture steadily, but significantly, declined from the average of 60.6% at DIV3 to 29.5% at DIV20 (Figure 2G). Despite the glial proliferation, long-term cultivation was achieved, with the longest maintained culture surviving past DIV72.

Electrophysiological Properties of Neurons Mature by DIV16

To describe the maturation process of embryonic spinal cord culture on the functional level, electrophysiological properties of neurons were recorded using patch-clamp technique in the whole-cell configuration at four timepoints: DIV2, DIV9, DIV16, and DIV24.

The E_m is considered a general characteristic of mature neurons (Sun et al., 2018). Average E_m of neurons significantly decreased from -55 ± 12.2 mV and -51.1 ± 10 mV at DIV2 and DIV9, respectively, to -59.6 ± 8.8 mV at DIV16 ($p = 0.01$ and $p = 0.006$) and to -59.9 ± 7.1 mV at DIV24 ($p = 0.009$ and $p < 0.001$) (Figure 3A), a figure consistent with mature interneurons. No further significant shift in E_m was observed between the neurons cultured for 16 and 24 days.

The IR is inversely proportional to the number of open ion channels and the size of the cell. A decrease in IR has been routinely used as an indicator of maturation of neurons in previous studies (Takazawa et al., 2012; Kopach et al., 2020). The average IR of studied neurons dropped significantly from $1,832 \pm 591.7$ M Ω at DIV2 to 817 ± 224.7 M Ω at DIV9 ($p = 0.021$) (Figure 3B). At later timepoints, IR values of 392.7 ± 111.1 M Ω at DIV16 and 387.3 ± 79.39 M Ω at DIV 24 were not significantly decreased, compared to IR at DIV9.

Cell size increased during development due to growth of the cells, which is why total C_m , a physical quantity directly proportional to the membrane surface area, is a useful tool to assess changes in neuronal maturation in culture (Golowasch et al., 2009). We found that a statistically significant shift in C_m value occurred between DIV2 and DIV9, after which no significant changes ensued (Figure 3C). At DIV2, the average C_m was 6.63 ± 0.13 pF while at DIV9, it was 14.77 ± 5.09 pF ($p = 0.042$).

The I_{Na+} plays a significant role in the action potential amplitude and has been reported to change during differentiation of embryonic and human-induced pluripotent stem cells into

TABLE 2 | List of antibodies used for immunocytochemistry.

Primary antibodies				
Immunogen	Dilution	Manufacturer	Cat. #	
Chx10	1/100	Santa Cruz	sc-365519	
Doublecortin	1/200	Santa Cruz	sc-271390	
GDNF Receptor alpha 1	1/100	Abcam	ab8026	
Gephyrin	1/500	Synaptic systems	147111	
GFP	1/1,000	Thermo Fisher	A10262	
Homer 1	1/500	Synaptic systems	160003	
Lbx1	1/10,000	Prof. Dr. Carmen Birchmeier-Kohler's lab		
Lmx1b (guinea pig)	1/10,000	Prof. Dr. Carmen Birchmeier-Kohler's lab		
Lmx1b (rabbit)	1/10,000	Prof. Dr. Carmen Birchmeier-Kohler's lab		
Neurofilament 70 kDa	1/400	Sigma-Aldrich	MAB1615	
Parvalbumin	1/500	Synaptic systems	195002	
PAX2	1/200	Thermo Fisher	71–6,000	
PKC γ	1/100	Santa Cruz	sc-166385	
Tlx3 (guinea pig)	1/20,000	Prof. Dr. Carmen Birchmeier-Kohler's lab		
Tlx3 (rabbit)	1/10,000	Prof. Dr. Carmen Birchmeier-Kohler's lab		
VGAT	1/500	Synaptic systems	131008	
VGLUT 1	1/500	Synaptic systems	135011	
WFA	1/500	Sigma-Aldrich	L1516	
β III tubulin	1/1,000	Abcam	ab78078	
β II tubulin	1/1,200	Abcam	ab68193	

Secondary antibodies				
Immunogen	Fluorophore	Dilution	Manufacturer	Cat. #
Chicken IgY	Alexa Fluor 488	1/200	Thermo Fisher	A-11039
Guinea Pig IgG (H + L)	Alexa Fluor 546	1/200	Thermo Fisher	A-11074
Mouse IgG (H + L)	Alexa Fluor 633	1/200	Thermo Fisher	A-21052
Mouse IgG (H + L)	Alexa Fluor 594	1/200	Thermo Fisher	A-11032
Mouse IgG (H + L)	Alexa Fluor 488	1/200	Thermo Fisher	A-11001
Rabbit IgG (H + L)	Alexa Fluor 594	1/200	Thermo Fisher	A-11012
Rabbit IgG (H + L)	Alexa Fluor 546	1/200	Thermo Fisher	A-11035
Rabbit IgG (H + L)	Alexa Fluor 488	1/200	Thermo Fisher	A-11034
Rabbit IgG (H + L)	Alexa Fluor 405	1/200	Thermo Fisher	A-31556

neuronal cells (Song et al., 2013). At DIV9, neurons in our culture exhibited an average I_{Na+} of -785.4 ± 387.5 pA, which was significantly lower compared to DIV24 I_{Na+} of $-1,248 \pm 684.3$ pA ($p = 0.031$) (Figure 3D).

Neurons in primary cultures were reported to have little spontaneous activity in the initial stages of cultivation, however, they exhibit it in later stages during cultivation, corresponding with synapse formation (Norris et al., 2006). The fraction of neurons generating AP increased significantly between DIV2 and DIV9 ($p = 0.003$) (Figure 3E) and did not change significantly in more mature cultures.

Maturity Markers of Primary Cortical Cultures Are Regulated in Primary Spinal Cord Cultures

Koseki et al. (2017) identified maturity markers in embryonic cortical neuron *in vitro* model by RNA sequencing and confirmed by immunocytochemistry. NF70 is upregulated, while

DBC is downregulated during maturation of these cultures. To assess the maturation process of spinal cord cultures, we analyzed expression of above-mentioned markers using immunocytochemistry (Figure 4). We found that the greatest downregulation of DBC expression in our cultures was between DIV6 and DIV13 ($p = 0.011$). NF70 immunoreactivity increased most significantly at DIV20, compared to DIV3 ($p = 0.025$) and DIV6 ($p = 0.029$).

Cells in the Spinal Cord Culture Form Inhibitory and Excitatory Synapses

To investigate neuronal connectivity and network development in the culture, we investigated colocalization of pre-synaptic and post-synaptic markers using immunocytochemistry (Figure 5). The excitatory pre-synaptic marker, vesicular glutamate transporter 1 (VGLUT1), was colocalized with Homer1, a post-synaptic density protein, that has a role in directing glutamate receptors. The largest shift in colocalization of these two markers was detected between DIV7 and DIV15

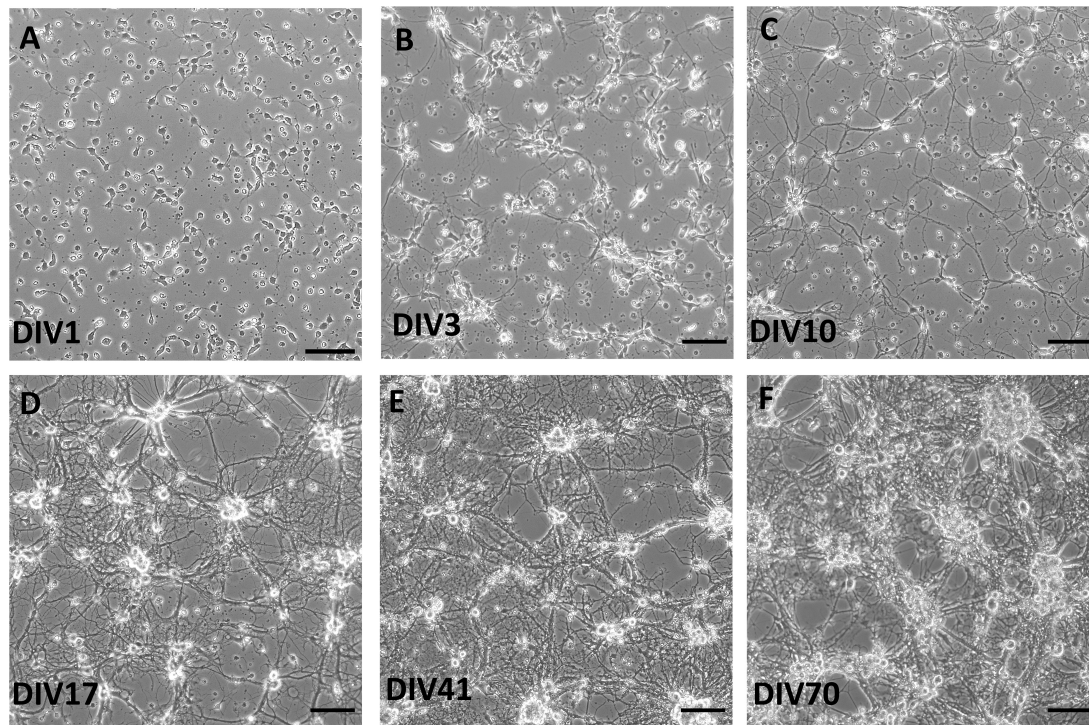


FIGURE 1 | Brightfield images of live spinal cord culture in day *in vitro* (DIV) 1 (A), DIV3 (B), DIV10 (C), DIV17 (D), DIV41 (E), and DIV70 (F). Growth of processes was observed already at DIV3, while more complex network occurred in older cultures, after DIV17. Scale bars: 50 μ m.

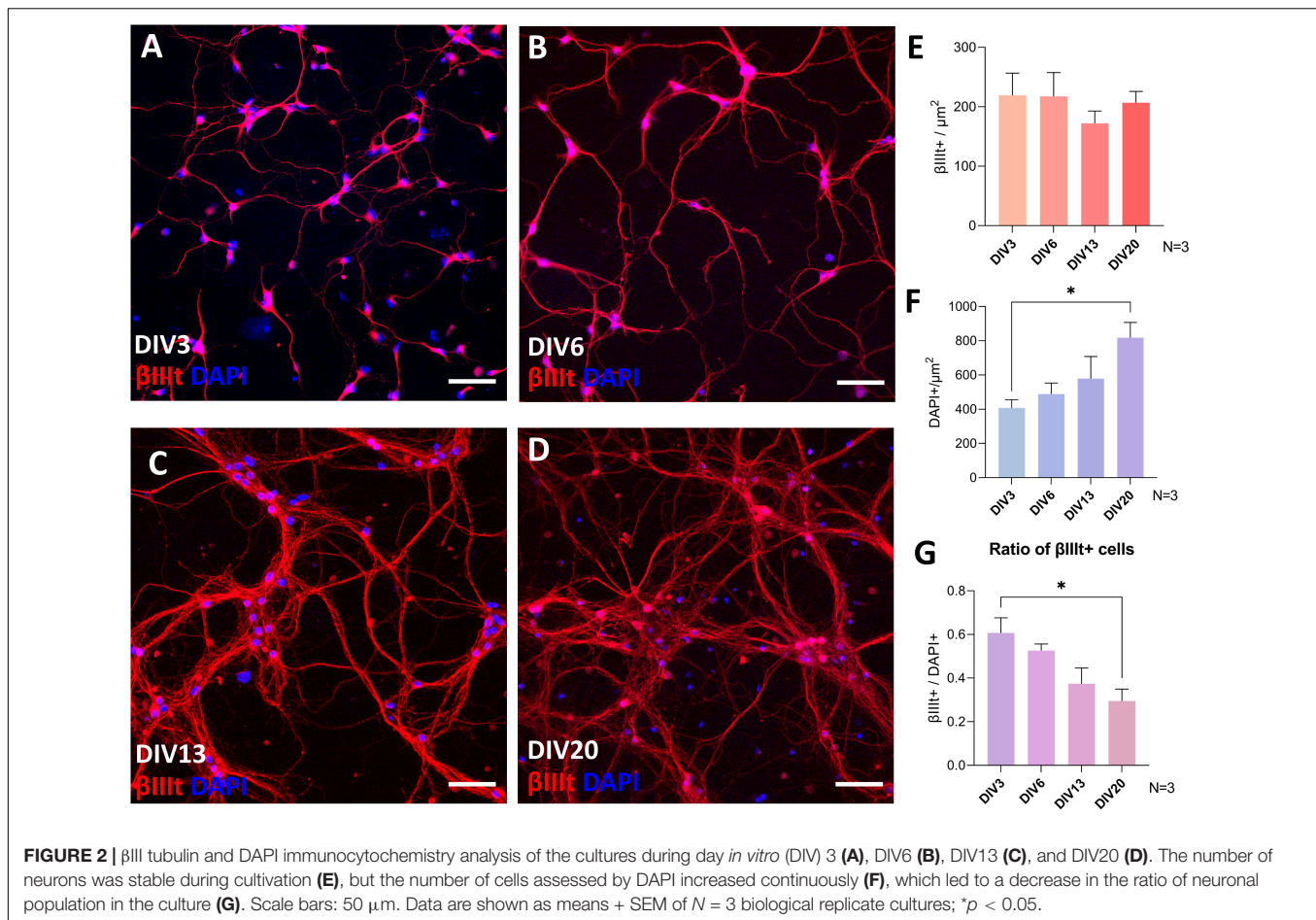
($p = 0.003$) (Figure 5C). After DIV15, we saw no significant increase in the colocalization of excitatory synapse markers. Regarding inhibitory synapses, colocalization of vesicular GABA transporter (VGAT) and gephyrin, a scaffold protein responsible for shaping the inhibitory postsynaptic density, was analyzed (Figure 5E). Similar to excitatory synapses, inhibitory synaptic marker colocalization increased significantly between DIV7 and DIV15 ($p = 0.043$). However, we also detected a significant increase in inhibitory synapse numbers between DIV15 and DIV28 ($p = 0.029$).

To assess whether the individual synaptic markers colocalize to differing extents during maturation, we analyzed the average ratio of co-localized synaptic puncta compared to total puncta counted for each individual synaptic marker (Figures 5D,F). We found that during cultivation, VGLUT1, Homer1, and VGAT colocalized in similar ratios, meaning that in immature and mature cultures, the same fraction of these synaptic markers did not colocalize with their counterpart synaptic marker. On the other hand, the gephyrin co-localized fraction was not as stable (Figure 5F). We detected an increase in the colocalized gephyrin fraction between DIV7 and DIV15 ($p = 0.005$).

Diverse Neuronal Markers Are Expressed in Primary Spinal Cord Culture

Utilizing immunocytochemistry in mature cultures, we confirmed that neurons express transcription factors associated

with particular types of spinal interneuron. Lbx1 (Figure 6A), Lmx1b (Figure 6B), Chx10 (Figure 6C), Tlx3, and Pax2 (Figure 6I) were expressed in differing proportions of neurons in our *in vitro* model. These transcription factors have been used as markers of neuronal classes in developing spinal cord (Alaynick et al., 2011; Lu et al., 2015). Counting the number of neurons stained by these markers, the most frequent markers in the culture were Pax2 and Tlx3. By counting Tlx3+ and Pax2+ nuclei of neurons identified by β III tubulin staining, we observed that Pax2 is expressed by approximately 28.5% of neurons and Tlx3+ by 24.3% of neurons in the culture on average and these values did not change significantly during cultivation (Figure 6H). Coexpression of both markers by the same cell was almost non-existent and the ratio of expression of both markers did not change significantly during maturation. Similarly, we estimated that 5.8% of neurons were Lbx1+ and 35.3% of neurons were Lmx1b+ at DIV17. Chx10+ neurons were sparsely present in the culture at DIV20, on average 30 cells per coverslip. Some motoneurons identified by ChAT staining were present in the culture in the first few days of the culture (data not shown), however, none of them survived during long-term cultivation. Next, we confirmed that subsets of neurons in the culture expressed protein kinase C gamma (PKC γ) (Figure 6D), parvalbumin (PV) (Figure 6F) at DIV20, and GDNF family receptor alpha-1 (GFR α 1) at DIV 17 (Figure 6E). These three proteins were expressed by the majority of neurons in the culture. *Wisteria floribunda* agglutinin (WFA) staining around neuronal cell bodies and dendrites identifies perineuronal nets (PNNs).



Neurons expressing perineuronal nets were only observed in exceptionally aged cultures (Figure 6G). At DIV72, we observed on average 23.5 WFA+ neurons per coverslip.

Neurons in Primary Culture Have Distinct Morphologies

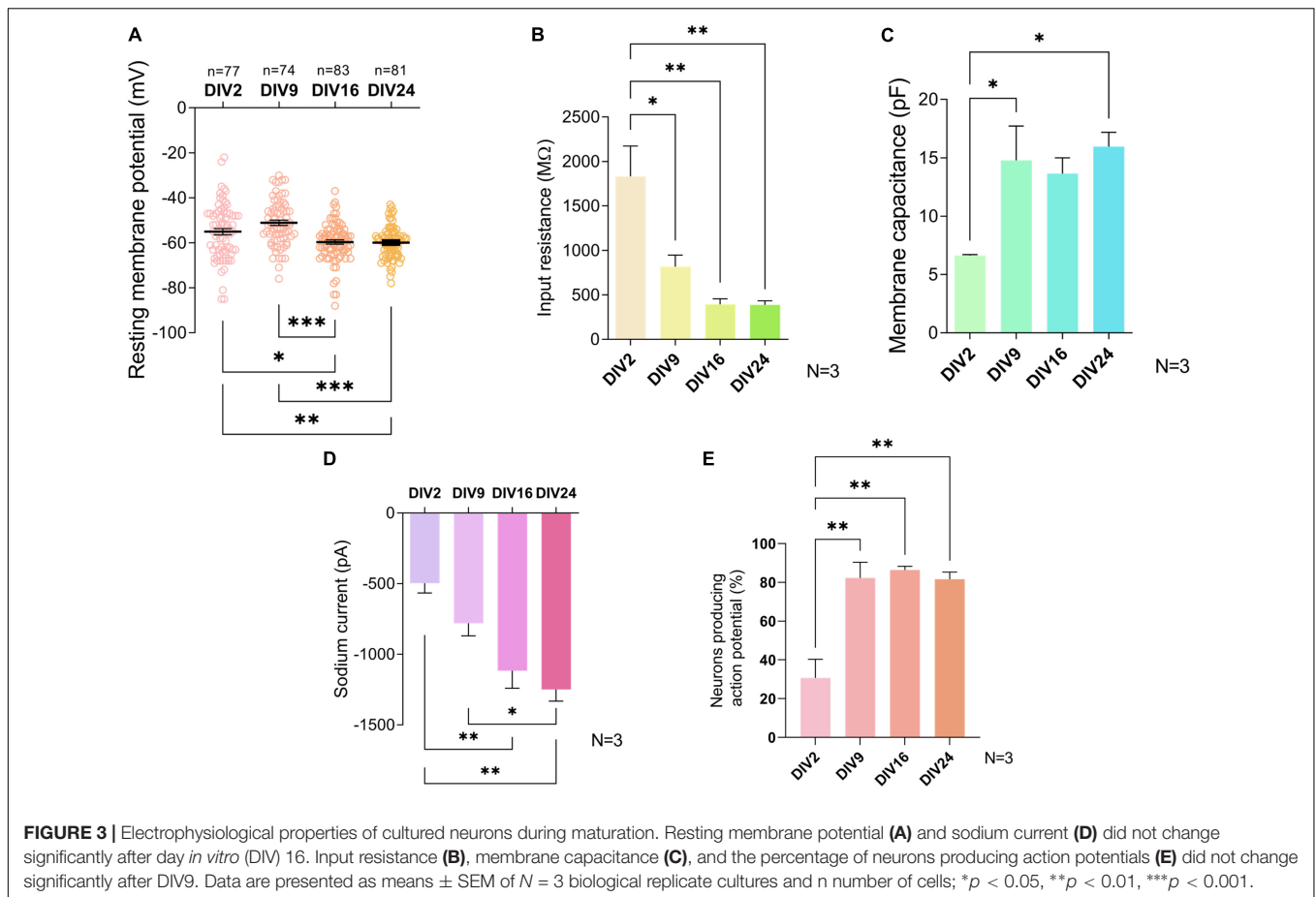
To investigate the morphology of neurons present in the culture, we transfected the cultures with GFP at DIV3 using a low transfection efficiency protocol. This resulted in expression of GFP by only a few cells on the coverslip, whose morphology could then be studied. The number and length of processes and their branches were analyzed with the SNT plugin in Fiji. DIV7-8 cells were sorted into three groups, simple, intermediate, and branched, based on the number of processes (Figure 7A and Table 3). Successful separation of the groups was confirmed by significant differences of multiple morphological parameters between the groups. In older cultures, at DIV14-15 (Figure 7B), DIV21-22 (Figure 7C), and DIV28-29 (Figure 7D), cable length (sum length of all analyzed processes) was identified as a better parameter for segregating morphologies. Morphologies identified in these timepoints were named small, medium, and large, but in all three DIVs, the range of cable length in each group was slightly different (Table 3).

In an effort to identify neuronal subtypes that these distinct morphologies belong to, we costained the GFP expressing neuronal cultures for Pax2 and Tlx3 (data not shown). We chose these markers because they were expressed by a large portion of neurons in the culture and because they allowed us to identify two different types of interneurons. We found that there were no clear differences between the morphologies of Pax2+ and Tlx3+ neurons at any of the analyzed time points of cultivation.

Comparison of morphological parameters of all neurons at different maturation stages revealed marked changes in the morphology of the neurons between DIV7-8 and DIV14-15 (Figure 8). The majority of the studied parameters did not significantly change after DIV15, except for the sum of all processes (cable length) and the sum of axonal branches. This indicates that even in older cultures, neuronal processes continue to grow.

Regenerative Capacity of Axons Decreases With Maturity

To characterize the regenerative capacity of neurons in the cultures, axons of individual cells at DIV7, 16, and 23 were cut using a 900 nm laser and observed over 14 h. Individual cells and their processes were visualized utilizing low-efficiency GFP transfection at DIV3. After the cut, cells either died or managed



to close the damaged area and form a characteristic retraction bulb—a swollen structure at the tip of the axon still attached to the cell (Figure 9A). The maturity of neurons did not affect the percentage of dead cells following the injury, which varied between 6–25% across individual experiments.

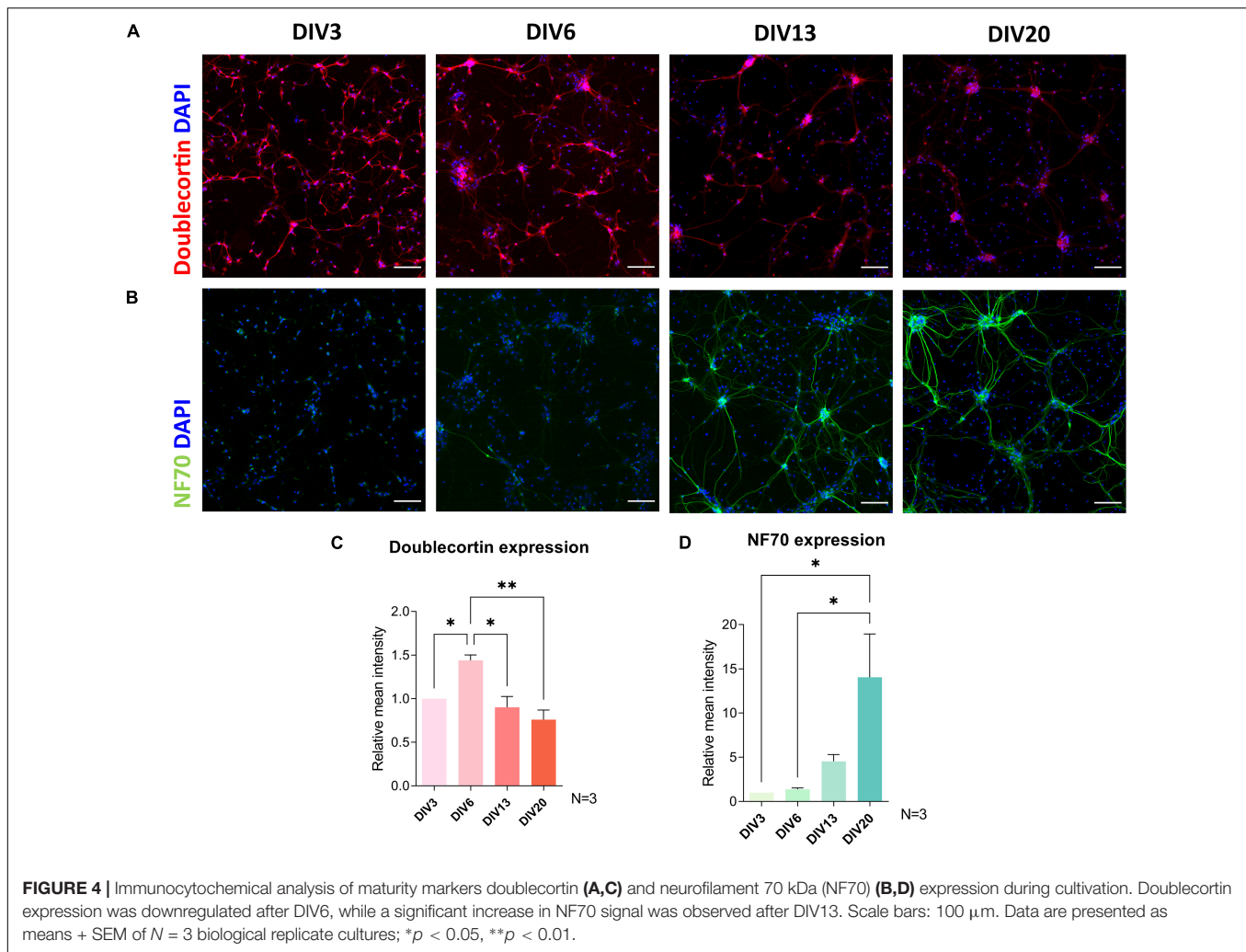
Formation of the retraction bulb sometimes occurred right next to the site of injury, or there was more retraction, and the retraction bulb formed further up the axons (Figure 9F). The time needed for formation of the retraction bulb was also variable. These two parameters—retraction distance and bulb formation time—were found to be significantly different in young neurons at DIV7, compared to DIV16 and DIV23 neurons (Figures 9B,C). In DIV7 neurons retraction distance was $31 \pm 16.81 \mu\text{m}$, while the bulb formation time was on average 1.7 ± 1.6 h. At DIV16, retraction distance was longer, at $40.6 \pm 28.1 \mu\text{m}$, while bulb formation time of 3.8 ± 2.7 h was prolonged significantly ($p = 0.004$). DIV23 neurons had both significantly longer retraction distance ($56.1 \pm 43.5 \mu\text{m}$) and bulb formation time (4 ± 2.2 h), compared to DIV7 ($p = 0.02$ and $p = 0.002$). Correlation analysis of all cells at all time points revealed a positive correlation between retraction distance and bulb formation time ($p < 0.001$) (Figure 9D), which indicates that longer retraction leads to slower sealing of the axon tip.

After successful bulb formation, the axons either initiated regeneration by forming a growth cone or failed to regenerate.

Failure of regeneration increased with maturity of the culture (Figure 9E). While at DIV7, 59.3% of axotomized neurons regenerated, only 25% regenerated at DIV16; no regenerating axons were observed at DIV23. In regenerating axons, initiation time, the time between retraction bulb and growth cone formation, was also evaluated (Figure 9F). We observed that regenerating DIV16 cells had longer initiation time compared to DIV7 neurons ($p = 0.02$). The speed of regeneration (length of newly synthesized axon in 2 h after initiation time) was lower at DIV7, although not significantly (Figure 9G).

DISCUSSION

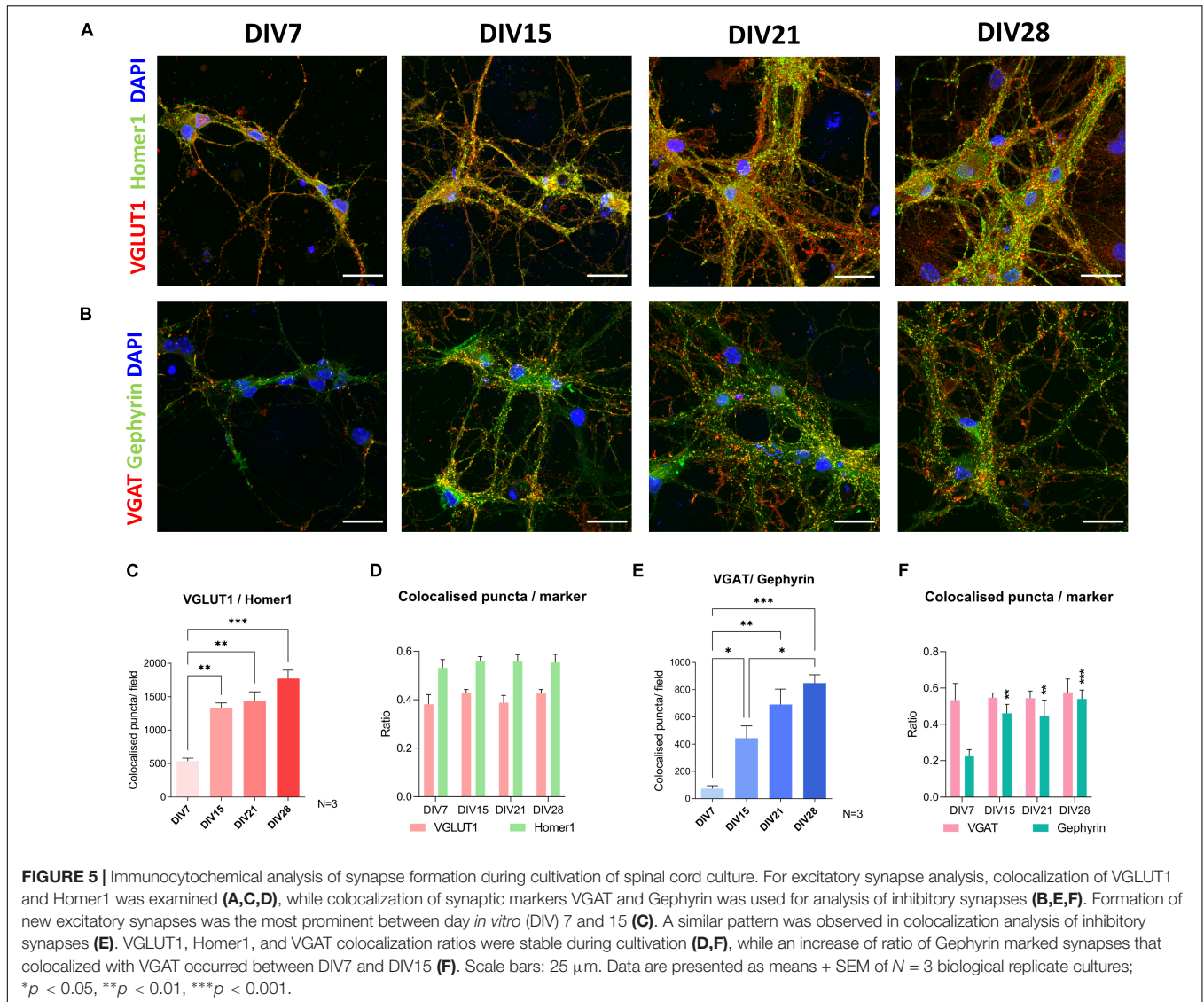
In the present study, we optimized a method of culturing primary spinal cord neurons, investigated their growth and maturation, and tested their regenerative ability. The cultures are robust, able to survive long term (>2 months), and are maintained in defined, simple serum-free medium. With increasing time in culture, we observed proliferation of glia. The use of anti-mitotic agents, such as 5-Fluoro-2'-deoxyuridine (FdU) and arabinosylcytosine C (AraC) has been routinely used previously in primary neuronal cultures to eradicate dividing cells (Stahl et al., 2007; Roppongi et al., 2017). However, their use in long-term cultivation has been reported to be problematic. It can lead



to death of neurons through glutamate excitotoxicity (Ahlemeyer et al., 2003), oxidative stress (Geller et al., 2001), or neurotrophic factor deprivation (Martin et al., 1990). On top of that, glial cells have been shown to be a crucial factor in synaptogenesis and in recreating complex functionality of the CNS in an *in vitro* system (Allen and Barres, 2005; Hui et al., 2016; Enright et al., 2020). For these reasons, we excluded the use of anti-mitotic agents in our culture, which led to proliferation of glia but did not affect the survival of neurons and probably encouraged neuronal maturation (Figure 2).

Our goal was to create a culture of spinal cord neurons that models the maturing and mature CNS and which is suitable for future experiments designed to enhance the ability of the neurons to regenerate. The viability of embryonic neuronal cultures is a great advantage in culture preparation, but the immaturity of the neurons after seeding is a problem as they display entirely different properties compared to mature neurons that have lost their intrinsic ability to regenerate (LaBarbera et al., 2021). To evaluate the maturity of our cultures, we investigated the expression of DBC, NF70, synaptic development, and electrophysiological properties of neurons during cultivation.

The alterations in the electrophysiological properties are hallmarks of neurodevelopment of spinal cord neurons (Durand et al., 2015) and have been used to stage neuronal maturation in cortical cultures (Koseki et al., 2017). The electrophysiological properties of neurons in our culture showed the typical changes associated with maturation until DIV16 after which there was no further change (Figure 3). In more detail, the major shift in most parameters in our functional studies already transpired before DIV9. Comparing these parameters to the electrical activity of neurons in P6-10 spinal cord slices recorded in a previous study by Sun and Harrington (2019), it can be argued that our neuronal culture is composed solely of interneurons. Interneurons in the cited study had high IR ($305 \pm 33 \text{ M}\Omega$), E_m of $-54.2 \pm 1 \text{ mV}$, and 65% of them exhibited spontaneous activity, which helped in distinguishing interneurons from motoneurons. Actual postnatal maturity of the neurons in the culture is difficult to assess using electrophysiological properties. We compared the properties in our cells with spinal cord slice recordings of P6-14 mice (Wilson et al., 2005; Sun and Harrington, 2019) and P0-3 whole cord recordings (Zhong et al., 2006). While some parameters, such

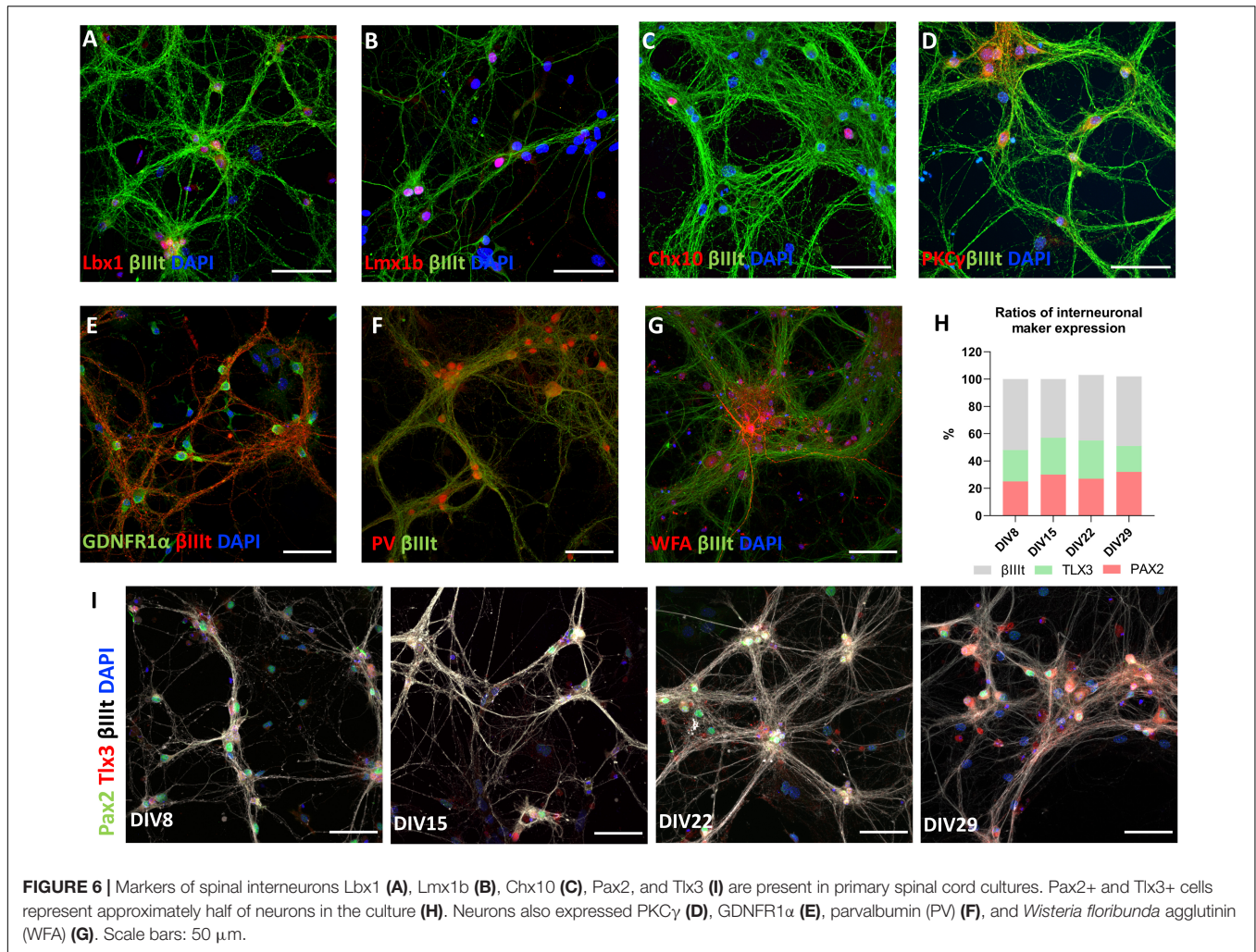


as E_m , were comparable to neurons of P0-3 spinal cord, other properties such as IR and percentage of spontaneously firing neurons indicated that our neurons were more mature at DIV16 than those of the P4-16 spinal cords. These results suggest that our cultures at around DIV16 exhibit electrical properties of early to late postnatal neurons.

DBC is a microtubule-associated protein expressed by migrating neurons during development. It has been used as a marker of neuronal precursors (Ayanlaja et al., 2017), while its downregulation has been reported in mature neurons (Brown et al., 2003). Developmental regulation of DBC was also observed *in vivo*. In mouse embryonic extracts, DBC expression is absent at E10.5, but present from E12.5 to newborn. Although DBC expression is still present in neonatal mouse brain, it is absent in adult mice (Francis et al., 1999). We observed a significant decrease in DBC immunoreactivity after DIV6 of culture (Figure 4). NF70 has been previously used as a mature axonal marker (Lu et al., 2017). NF70 mRNA analysis in embryonic and

early postnatal mouse spinal cords shows, that this transcript is present already in E13. The expression is downregulated until E18 and then starts to increase until postnatal day 21 (Pernas-Alonso et al., 1996). In our cultures, there was a sharp upregulation of this marker at DIV20. Maturity of the culture was also confirmed by observing the formation of neural networks (Figure 5). The number of excitatory and inhibitory synapses was increasing during the first 2 weeks of culture, after which they plateaued, which was previously observed to occur in cultures of primary cortical and striatal neurons between DIV14 and DIV21 (Moutaux et al., 2018).

Although there is no consensus of neuronal subtypes classification in adult spinal cord, there have been several recent studies that tackled this problem in various approaches (Zeng and Sanes, 2017; Hayashi et al., 2018; Dobrott et al., 2019). The most efficient way is to classify cell types by molecular markers- proteins expressed by only specific cell groups. Transcription factors have been used to classify spinal neurons,



as they control neuronal specialization during development (Lu et al., 2015; Russ et al., 2021). Although the expression of the transcription factors can be transient- their expression is decreased after differentiation (Gosgnach et al., 2017), some continue to be expressed during adulthood (Del Barrio et al., 2013). We identified expression of several of these transcription factors in our cultures, namely Lbx1, Lmx1b, Chx10, Pax2, and Tlx3 (Figure 6). Lbx1 transcription factor participates in differentiation of dorsal horn neurons (Müller et al., 2002), it is expressed by laminae III-IV neurons of adult spinal cord, which are mostly excitatory, but not exclusively. Lmx1b+ neurons also express Lbx1, but they are only excitatory and expressed at high levels in laminae I-III (Del Barrio et al., 2013). Lmx1b+ neurons in our cultures were colocalized with majority of Tlx3 neurons (data not shown), which was also previously confirmed *in vivo* (Dai et al., 2008). Tlx3 transcription factor, present mostly in laminae I-II, has been identified to have direct control in specifying excitatory neurons in the dorsal horn (Monteiro et al., 2021). Apart from the previously mentioned, mostly excitatory, interneurons, we have also observed a large population of Pax2+ neurons in our cultures. Pax2 is essential for the

differentiation of GABAergic neurons and its expression has been used as a marker of inhibitory neurons in the mouse dorsal horn (Larsson, 2017). The presence of ventral interneurons was also confirmed using Chx10 staining. Chx10 has been used as a marker of V2a excitatory interneurons in the ventral spinal cord, which participate in control of the limbs (Hayashi et al., 2018). In addition to transcription factors, other proteins have also been used to classify neurons in adult spinal cord. PKCγ is one such protein that is expressed by excitatory interneurons in lamina II that participate in mechanical and thermal allodynia (Neumann et al., 2008). Parvalbumin, on the other hand, is a marker of inhibitory interneurons, both GABAergic and glycinergic, located between the lamina II and III, which act as filters of low-threshold mechanoreceptive inputs (Petitjean et al., 2015; Häring et al., 2018). Both PKCγ and PV were expressed by our neuronal cultures. We found that ChAT positive cells do not survive long in the described culture. Motor neurons are known to be particularly vulnerable and rely heavily on trophic support of peripherally connected cells, such as muscle cells and Schwann cells for survival (Bucchia et al., 2018). The loss of trophic support after dissection could have eventually led to death

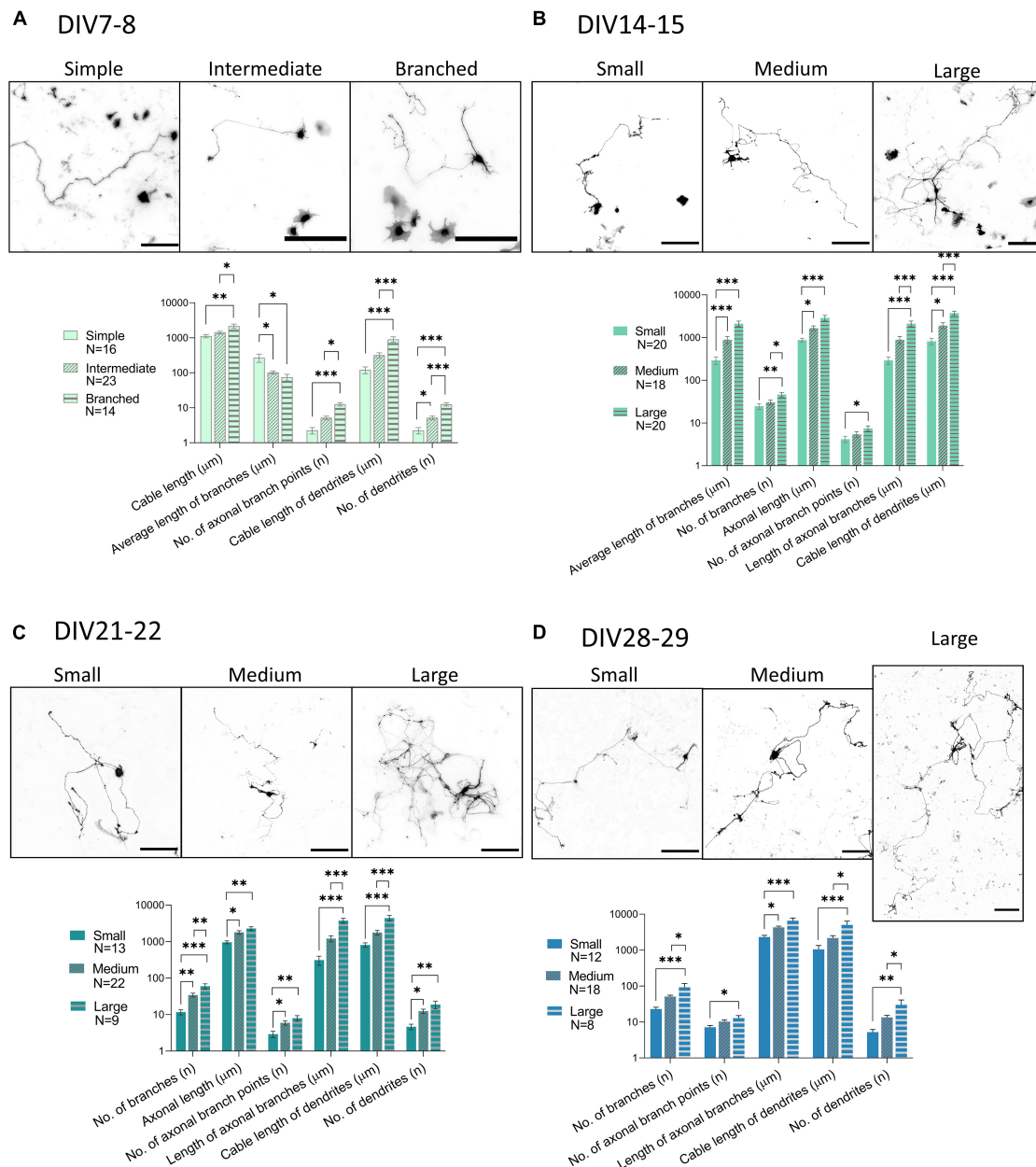


FIGURE 7 | Morphological groups of neurons transfected with GFP (black) during various days *in vitro* (DIV), DIV7-8 (A), DIV14-15 (B), DIV21-22 (C), DIV28-29 (D). While DIV7 neurons were successfully categorized according to the number of processes into simple, intermediate, and branched, from DIV14 onward, the length of processes was found to be a better parameter for segregating morphologies into small, medium, and large. Scale bars: 200 μm. One-way ANOVA with Turkey's *post hoc* test was used for analyzing the difference between morphological groups. Data are presented as means + SEM of N number of cells from 3 biological replicates; * $p < 0.05$, ** $p < 0.01$, *** $p < 0.001$.

of motor neurons in our cultures. Due to the lack of specific markers, we can only speculate if projection neurons shared the same fate. Projection neurons represent a very small portion (<1%) of neurons of the dorsal horn. They are located in lamina I and dispersed throughout lamina III–VI (Abraira and Ginty, 2013). The majority of projection neurons retrogradely traced by cholera toxin B subunit (CTb) were found to express neurokinin 1 receptor (NK1r) (Spike et al., 2003; Cameron et al., 2015), but a

big portion of lamina I, IV, V and VI neurons, therefore mostly interneurons, express this receptor as well (Todd et al., 1998). NK1r immunostaining alone is therefore not sufficient to prove the presence of projection neurons.

To analyze the morphology of neurons during maturation and to attempt to classify them into characteristic groups, we measured the length and number of their processes. Previous studies classified the spinal cord neuron morphology according

TABLE 3 | Morphological groups of neurons identified during cultivation of spinal cord cultures.

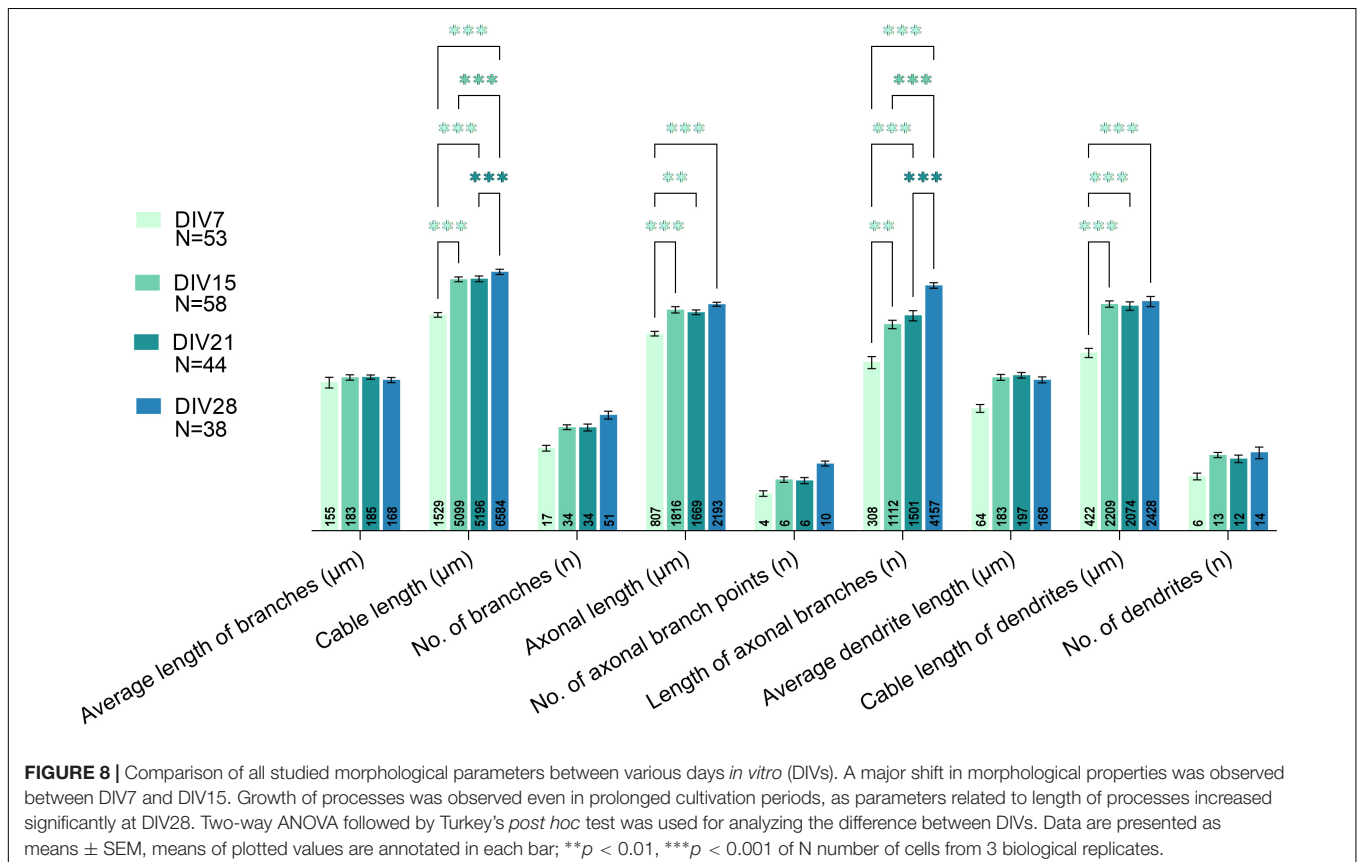
	Morphological group	Range	N	N total
DIV7-8	Simple	1–9 b	16	53
	Intermediate	10–19 b	23	
	Branched	20–58 b	14	
DIV15-16	Small	300–3,000 μm	20	58
	Medium	3,000–6,000 μm	18	
	Large	6,000–13,000 μm	20	
DIV21-22	Small	900–3,000 μm	13	44
	Medium	3,000–7,500 μm	22	
	Large	7,500–14,000 μm	9	
DIV28-29	Small	1,700–4,500 μm	12	38
	Medium	4,500–8,000 μm	18	
	Large	8,000–20,000 μm	8	

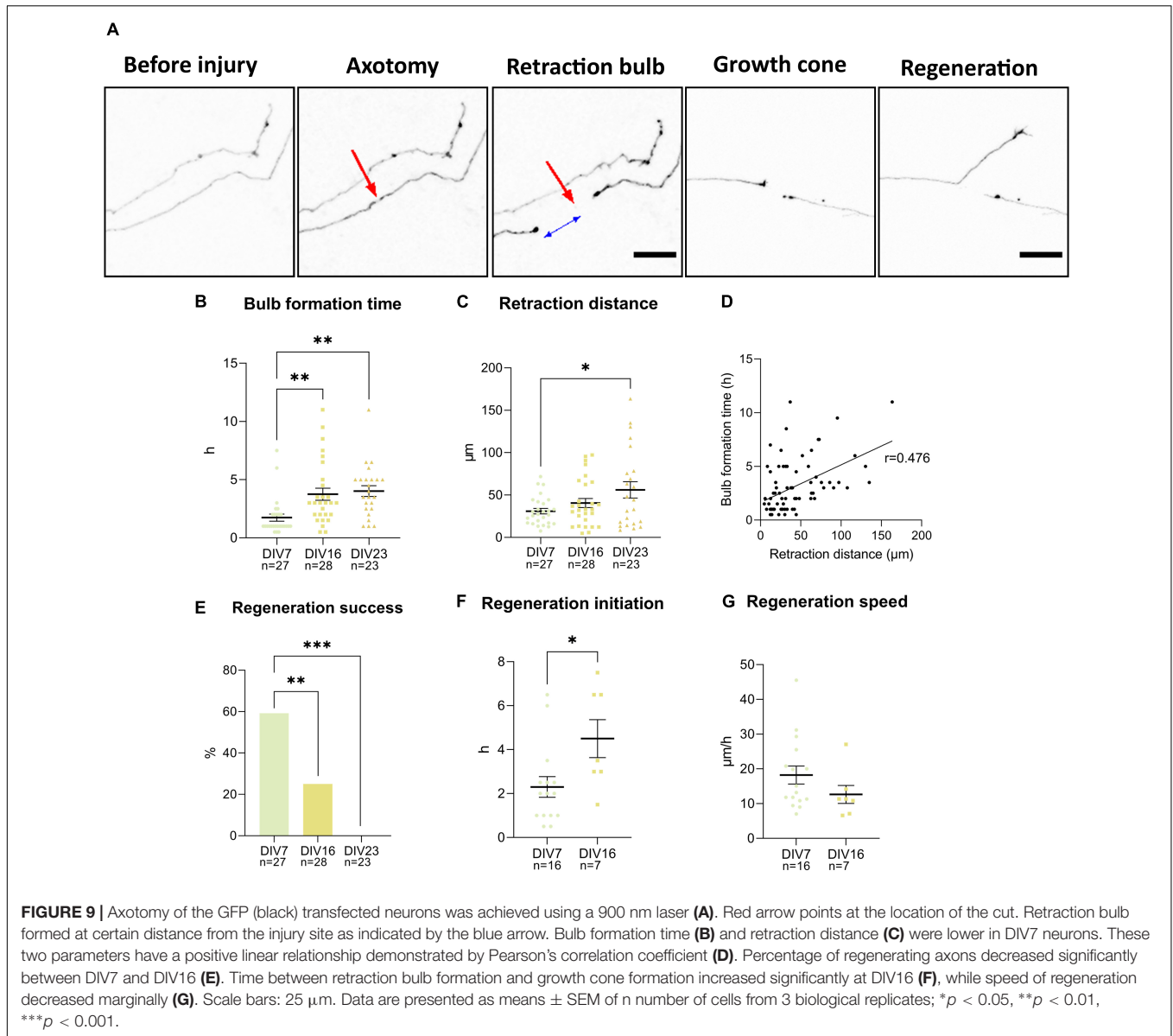
DIV7-8 neurons were separated according to the number of branches (b), while older neurons were grouped according to the sum length of their processes.

to laminar location, particular geometry, and neurite orientation (Grudt and Perl, 2002; Hantman et al., 2004), which is not possible *in vitro*. Gertz et al. (2010) reported increasing length and number of neurites of spinal cord motoneurons during cultivation, but 48 h. We analyzed the morphology parameters in the course of 4 weeks *in vitro*, during which we distinguished individual morphologies and observed growth of processes

even in older cultures. The morphological groups that were identified were not characteristic of either Tlx3+ or Pax2+ cells, which are markers of two different interneuronal subtypes. Electrophysiological characteristics of the morphological groups were not assessed. Additionally, we observed that even in older cultures, neuronal processes continue to grow (Figure 8). Electrophysiological parameters IR and C_m correlate with cell size (Sun et al., 2018), but we did not see changes in these parameters after DIV9 (Figures 3B,C). It is important to note, that the morphological changes in older cultures were identified at DIV28, while the oldest cultures recorded by patch-clamp were at DIV24, which could be the reason for this inconsistency. On the other hand, we observed an increase in the number of synapses at DIV28 (Figure 5), which could indicate that elongation of the processes observed at the same timepoint in morphology analysis is due to formation of new connections between neurons in the culture.

By following events that occurred after axotomy of spinal cord neurons, we observed that more mature cells react more slowly to laser-induced injury and retract further from the injury site compared to younger cells (Figure 9). By DIV23, neurons lost all regenerative capacity and even at DIV16, the axon regeneration was slower. These results indicate that spinal neurons lose their regenerative capacity during maturation *in vitro*, similarly to cortical cultures, as was shown before (Koseki et al., 2017). We observed a similar transition in neuronal properties in other experiments around





this time point as well. The major shift in morphology during *in vitro* maturation was observed between DIV7 and DIV15 (Figure 8). The same cultivation period was critical in changes of maturity marker expressions, synaptic connectivity, and most of the electrophysiological properties. These results indicate that major intrinsic maturation events are occurring at this time point in the cultured neurons. Loss of plasticity and regenerative ability in CNS neurons during development *in vivo* is well established (Fawcett, 2020). Apart from the inhibitory environment that is created at the injury site, mature neurons themselves lack intrinsic regenerative properties. During the loss of regenerative ability, neurons show changes in expression of growth-related molecules, and they also become polarized into somatodendritic and axonal domains. Axons alone lack molecules such as growth-related receptors, as well as mechanisms deemed vital for regeneration (Kappagantula

et al., 2014; Franssen et al., 2015; Cheah et al., 2016). Apart from non-regenerating axons, CNS neurons do not express the regenerative program that is seen with the upregulation of many genes that is initiated after injury of peripheral nerves (Ben-Yaakov et al., 2012).

In conclusion, we developed, validated, and described a new culture of spinal cord neurons. We believe that the described culture efficiently models the biology of the spinal cord, which makes it a valuable tool for future studies.

DATA AVAILABILITY STATEMENT

The original contributions presented in the study are included in the article/supplementary material, further inquiries can be directed to the corresponding author/s.

ETHICS STATEMENT

All cell isolations from mice embryos were performed in accordance with the European Communities Council Directive of 22.09.2010 (2010/63/EU) regarding the use of animals in research and were approved by the Ethics Committee of the Institute of Experimental Medicine ASCR, Prague, Czechia under no. 54/2017 (approved 14.10.2017 and valid till 31.07.2022).

AUTHOR CONTRIBUTIONS

IV drafted the manuscript, performed and analyzed all experiments, except patch-clamp recordings, which were performed by JK, JCK, JF, and PJ conceived of the project and supervised the experiments. All authors contributed to editing the manuscript.

REFERENCES

- Abraira, V. E., and Ginty, D. D. (2013). The sensory neurons of touch. *Neuron* 79, 618–639. doi: 10.1016/j.neuron.2013.07.051
- Abu-Rub, M., McMahon, S., Zeugolis, D. I., Windebank, A., and Pandit, A. (2010). Spinal cord injury in vitro: modelling axon growth inhibition. *Drug Discov. Today* 15, 436–443. doi: 10.1016/j.drudis.2010.03.008
- Ahlemeyer, B., Kölker, S., Zhu, Y., Hoffmann, G. F., and Kriegstein, J. (2003). Cytosine arabinofuranoside-induced activation of astrocytes increases the susceptibility of neurons to glutamate due to the release of soluble factors. *Neurochem. Int.* 42, 567–581. doi: 10.1016/s0197-0186(02)00164-x
- Alaynick, W. A., Jessell, T. M., and Pfaff, S. L. (2011). SnapShot: spinal cord development. *Cell* 146, 178.e–178.e. doi: 10.1016/j.cell.2011.06.038
- Allen, N. J., and Barres, B. A. (2005). Signaling between glia and neurons: focus on synaptic plasticity. *Curr. Opin. Neurobiol.* 15, 542–548. doi: 10.1016/j.conb.2005.08.006
- Anderson, M. A., Burda, J. E., Ren, Y., Ao, Y., O’Shea, T. M., Kawaguchi, R., et al. (2016). Astrocyte scar formation aids central nervous system axon regeneration. *Nature* 532, 195–200. doi: 10.1038/nature17623
- Anderson, M. A., O’Shea, T. M., Burda, J. E., Ao, Y., Barlately, S. L., Bernstein, A. M., et al. (2018). Required growth facilitators propel axon regeneration across complete spinal cord injury. *Nature* 561, 396–400. doi: 10.1038/s41586-018-0467-6
- Arshadi, C., Günther, U., Eddison, M., Harrington, K. I. S., and Ferreira, T. A. (2020). SNT: A Unifying Toolbox for Quantification of Neuronal Anatomy. *Neuroscience. Nat. Methods* 18, 374–377. doi: 10.1101/2020.07.13.179325
- Ayanlaja, A. A., Xiong, Y., Gao, Y., Ji, G., Tang, C., Abdikani Abdullah, Z., et al. (2017). Distinct Features of Doublecortin as a Marker of Neuronal Migration and Its Implications in Cancer Cell Mobility. *Front. Mol. Neurosci.* 10:199. doi: 10.3389/fnmol.2017.00199
- Barbati, A. C., Fang, C., Banker, G. A., and Kirby, B. J. (2013). Culture of primary rat hippocampal neurons: design, analysis, and optimization of a microfluidic device for cell seeding, coherent growth, and solute delivery. *Biomed. Microdevices* 15, 97–108. doi: 10.1007/s10544-012-9691-2
- Bareyre, F. M., Kerschensteiner, M., Raineteau, O., Mettenleiter, T. C., Weinmann, O., and Schwab, M. E. (2004). The injured spinal cord spontaneously forms a new intraspinal circuit in adult rats. *Nat. Neurosci.* 7, 269–277. doi: 10.1038/nn1195
- Ben-Yaakov, K., Dagan, S. Y., Segal-Ruder, Y., Shalem, O., Vuppalandhi, D., Willis, D. E., et al. (2012). Axonal transcription factors signal retrogradely in lesioned peripheral nerve. *EMBO J.* 31, 1350–1363. doi: 10.1038/emboj.2011.494
- Blesch, A., Fischer, I., and Tuszynski, M. H. (2012). Gene therapy, neurotrophic factors and spinal cord regeneration. *Handb. Clin. Neurol.* 109, 563–574. doi: 10.1016/B978-0-444-52137-8.00035-8
- Brown, J. P., Couillard-Després, S., Cooper-Kuhn, C. M., Winkler, J., Aigner, L., and Kuhn, H. G. (2003). Transient expression of doublecortin

FUNDING

This work was supported by Operational Program Research, Development, and Education in the framework of the project “Center of Reconstructive Neuroscience,” registration number CZ.02.1.01/0.0/0.0/15_003/0000419. We acknowledge the core facility IMCF BIOCEV, supported by the MEYS CR (LM2018129 Czech-Biolmaging) for their support with obtaining scientific data presented in this manuscript.

ACKNOWLEDGMENTS

We would like to thank Carmen Birchmeier-Kohler and Thomas Müller from Max-Delbrueck Center for Molecular Medicine, Berlin, Germany for proving us with antibodies against Tlx3, Lbx1, and Lmx1b.

- during adult neurogenesis. *J. Comp. Neurol.* 467, 1–10. doi: 10.1002/cne.10874
- Bucchia, M., Merwin, S. J., Re, D. B., and Kariya, S. (2018). Limitations and Challenges in Modeling Diseases Involving Spinal Motor Neuron Degeneration in Vitro. *Front. Cell. Neurosci.* 12:61. doi: 10.3389/fncel.2018.00061
- Cameron, D., Polgár, E., Gutierrez-Mecinas, M., Gomez-Lima, M., Watanabe, M., and Todd, A. J. (2015). The organisation of spinoparabrachial neurons in the mouse. *Pain* 156, 2061–2071. doi: 10.1097/j.pain.0000000000000270
- Cheah, M., Andrews, M. R., Chew, D. J., Moloney, E. B., Verhaagen, J., Fässler, R., et al. (2016). Expression of an Activated Integrin Promotes Long-Distance Sensory Axon Regeneration in the Spinal Cord. *J. Neurosci.* 36, 7283–7297. doi: 10.1523/JNEUROSCI.0901-16.2016
- Courtine, G., Song, B., Roy, R. R., Zhong, H., Herrmann, J. E., Ao, Y., et al. (2008). Recovery of supraspinal control of stepping via indirect propriospinal relay connections after spinal cord injury. *Nat Med* 14, 69–74. doi: 10.1038/nm1682
- Dai, J.-X., Hu, Z.-L., Shi, M., Guo, C., and Ding, Y.-Q. (2008). Postnatal ontogeny of the transcription factor Lmx1b in the mouse central nervous system. *Journal of Comparative Neurology* 509, 341–355. doi: 10.1002/cne.21759
- Del Barrio, M. G., Bourane, S., Grossmann, K., Schüle, R., Britsch, S., O’Leary, D. D. M., et al. (2013). A transcription factor code defines nine sensory interneuron subtypes in the mechanosensory area of the spinal cord. *PLoS ONE* 8:e77928. doi: 10.1371/journal.pone.0077928
- Dobrott, C. I., Sathyamurthy, A., and Levine, A. J. (2019). Decoding cell type diversity within the spinal cord. *Curr. Opin. Physiol.* 8, 1–6. doi: 10.1016/j.cophys.2018.11.006
- Donaldson, K., and Höke, A. (2014). Studying axonal degeneration and regeneration using in vitro and in vivo models: the translational potential. *Fut. Neurol.* 9, 461–473. doi: 10.2217/fnl.14.29
- Durand, J., Filipchuk, A., Pambo-Pambo, A., Amendola, J., Borisovna Kulagina, I., and Guéritaud, J.-P. (2015). Developing electrical properties of postnatal mouse lumbar motoneurons. *Front. Cell. Neurosci.* 9:349. doi: 10.3389/fncel.2015.00349
- Eldeiry, M., Yamanaka, K., Reece, T. B., and Aftab, M. (2017). Spinal cord neurons isolation and culture from neonatal mice. *J. Vis. Exp.* 11:55856. doi: 10.3791/55856
- Enright, H. A., Lam, D., Sebastian, A., Sales, A. P., Cadena, J., Hum, N. R., et al. (2020). Functional and transcriptional characterization of complex neuronal co-cultures. *Sci. Rep.* 10:11007. doi: 10.1038/s41598-020-67691-2
- Fawcett, J. W. (2020). The Struggle to Make CNS Axons Regenerate: Why Has It Been so Difficult? *Neurochem. Res.* 45, 144–158. doi: 10.1007/s11064-019-02844-y
- Francis, F., Koukoulakoff, A., Boucher, D., Chafey, P., Schaar, B., Vinet, M.-C., et al. (1999). Doublecortin is a developmentally regulated, microtubule-associated protein expressed in migrating and differentiating neurons. *Neuron* 23, 247–256. doi: 10.1016/S0896-6273(00)80777-1

- Franssen, E. H. P., Zhao, R.-R., Koseki, H., Kanamarlapudi, V., Hoogenraad, C. C., Eva, R., et al. (2015). Exclusion of integrins from CNS axons is regulated by Arf6 activation and the AIS. *J. Neurosci.* 35, 8359–8375. doi: 10.1523/JNEUROSCI.2850-14.2015
- Geller, H. M., Cheng, K. Y., Goldsmith, N. K., Romero, A. A., Zhang, A. L., Morris, E. J., et al. (2001). Oxidative stress mediates neuronal DNA damage and apoptosis in response to cytosine arabinoside. *J. Neurochem.* 78, 265–275. doi: 10.1046/j.1471-4159.2001.00395.x
- Gertz, C. C., Leach, M. K., Birrell, L. K., Martin, D. C., Feldman, E. L., and Corey, J. M. (2010). Accelerated neurogenesis and maturation of primary spinal motor neurons in response to nanofibers. *Dev Neurobiol* 70, 589–603. doi: 10.1002/dneu.20792
- Golowasch, J., Thomas, G., Taylor, A. L., Patel, A., Pineda, A., Khalil, C., et al. (2009). Membrane capacitance measurements revisited: dependence of capacitance value on measurement method in nonisopotential neurons. *J. Neurophysiol.* 102, 2161–2175. doi: 10.1152/jn.00160.2009
- Gosgnach, S., Bikoff, J. B., Dougherty, K. J., Manira, A. E., Lanuza, G. M., and Zhang, Y. (2017). Delineating the Diversity of Spinal Interneurons in Locomotor Circuits. *J. Neurosci.* 37, 10835–10841. doi: 10.1523/JNEUROSCI.1829-17.2017
- Grudt, T. J., and Perl, E. R. (2002). Correlations between neuronal morphology and electrophysiological features in the rodent superficial dorsal horn. *J. Physiol.* 540, 189–207. doi: 10.1113/jphysiol.2001.012890
- Hantman, A. W., van den Pol, A. N., and Perl, E. R. (2004). Morphological and physiological features of a set of spinal substantia gelatinosa neurons defined by green fluorescent protein expression. *J. Neurosci.* 24, 836–842. doi: 10.1523/JNEUROSCI.4221-03.2004
- Häring, M., Zeisel, A., Hochgerner, H., Rinwa, P., Jakobsson, J. E. T., Lönnerberg, P., et al. (2018). Neuronal atlas of the dorsal horn defines its architecture and links sensory input to transcriptional cell types. *Nat. Neurosci.* 21, 869–880. doi: 10.1038/s41593-018-0141-1
- Hayashi, M., Hinkley, C. A., Driscoll, S. P., Moore, N. J., Levine, A. J., Hilde, K. L., et al. (2018). Graded Arrays of Spinal and Supraspinal V2a Interneuron Subtypes Underlie Forelimb and Hindlimb Motor Control. *Neuron* 97, 869–884.e5. doi: 10.1016/j.neuron.2018.01.023
- Hui, C. W., Zhang, Y., and Herrup, K. (2016). Non-Neuronal Cells Are Required to Mediate the Effects of Neuroinflammation: Results from a Neuron-Enriched Culture System. *PLoS One* 11:e0147134. doi: 10.1371/journal.pone.0147134
- Kaech, S., and Banker, G. (2006). Culturing hippocampal neurons. *Nat. Protoc.* 1, 2406–2415. doi: 10.1038/nprot.2006.356
- Kappagantula, S., Andrews, M. R., Cheah, M., Abad-Rodriguez, J., Dotti, C. G., and Fawcett, J. W. (2014). Neu3 Sialidase-Mediated Ganglioside Conversion Is Necessary for Axon Regeneration and Is Blocked in CNS Axons. *J. Neurosci.* 34, 2477–2492. doi: 10.1523/JNEUROSCI.4432-13.2014
- Kopach, O., Esteras, N., Wray, S., Rusakov, D. A., and Abramov, A. Y. (2020). Maturation and phenotype of pathophysiological neuronal excitability of human cells in tau-related dementia. *J. Cell. Sci.* 133, jcs241687. doi: 10.1242/jcs.241687
- Koseki, H., Donegá, M., Lam, B. Y., Petrova, V., van Erp, S., Yeo, G. S., et al. (2017). Selective rab11 transport and the intrinsic regenerative ability of CNS axons. *Elife* 6:e26956. doi: 10.7554/eLife.26956
- LaBarbera, K. M., Limegrover, C., Rehak, C., Yurko, R., Izzo, N. J., Knezovich, N., et al. (2021). Modeling the mature CNS: A predictive screening platform for neurodegenerative disease drug discovery. *J. Neurosci. Methods* 358:109180. doi: 10.1016/j.jneumeth.2021.109180
- Larsson, M. (2017). Pax2 is persistently expressed by GABAergic neurons throughout the adult rat dorsal horn. *Neurosci. Lett.* 638, 96–101. doi: 10.1016/j.neulet.2016.12.015
- Lu, D. C., Niu, T., and Alaynick, W. A. (2015). Molecular and cellular development of spinal cord locomotor circuitry. *Front. Mol. Neurosci.* 8:25. doi: 10.3389/fnmol.2015.00025
- Lu, P., Ceto, S., Wang, Y., Graham, L., Wu, D., Kumamaru, H., et al. (2017). Prolonged human neural stem cell maturation supports recovery in injured rodent CNS. *J. Clin. Invest.* 127, 3287–3299. doi: 10.1172/JCI92955
- Lu, P., Kadoya, K., and Tuszyński, M. H. (2014). Axonal growth and connectivity from neural stem cell grafts in models of spinal cord injury. *Curr. Opin. Neurobiol.* 27, 103–109. doi: 10.1016/j.conb.2014.03.010
- Martin, D., Wallace, T., and Johnson, E. (1990). Cytosine arabinoside kills postmitotic neurons in a fashion resembling trophic factor deprivation: evidence that a deoxycytidine-dependent process may be required for nerve growth factor signal transduction. *J. Neurosci.* 10, 184–193. doi: 10.1523/JNEUROSCI.10-01-00184.1990
- Martinez, M., Delivet-Mongrain, H., Leblond, H., and Rossignol, S. (2012). Incomplete spinal cord injury promotes durable functional changes within the spinal locomotor circuitry. *J. Neurophysiol.* 108, 124–134. doi: 10.1152/jn.00073.2012
- May, Z., Fenrich, K. K., Dahlby, J., Batty, N. J., Torres-Espin, A., and Fouad, K. (2017). Following Spinal Cord Injury Transected Reticulospinal Tract Axons Develop New Collateral Inputs to Spinal Interneurons in Parallel with Locomotor Recovery. *Neural Plasticity* 2017:1932875. doi: 10.1155/2017/1932875
- Monteiro, F. A., Miranda, R. M., Samina, M. C., Dias, A. F., Raposo, A. A. S. F., Oliveira, P., et al. (2021). Tlx3 Exerts Direct Control in Specifying Excitatory Over Inhibitory Neurons in the Dorsal Spinal Cord. *Front. Cell. Dev. Biol.* 9:642697. doi: 10.3389/fcell.2021.642697
- Moore, D. L., Blackmore, M. G., Hu, Y., Kaestner, K. H., Bixby, J. L., Lemmon, V. P., et al. (2009). KLF family members regulate intrinsic axon regeneration ability. *Science* 326, 298–301. doi: 10.1126/science.1175737
- Moutaux, E., Christaller, W., Scaramuzzino, C., Genoux, A., Charlot, B., Cazorla, M., et al. (2018). Neuronal network maturation differently affects secretory vesicles and mitochondria transport in axons. *Sci. Rep.* 8:13429. doi: 10.1038/s41598-018-31759-x
- Müller, T., Brohmann, H., Pierani, A., Heppenstall, P. A., Lewin, G. R., Jessell, T. M., et al. (2002). The homeodomain factor *lhx1* distinguishes two major programs of neuronal differentiation in the dorsal spinal cord. *Neuron* 34, 551–562. doi: 10.1016/s0896-6273(02)00689-x
- Neumann, S., Braz, J. M., Skinner, K., Llewellyn-Smith, I. J., and Basbaum, A. I. (2008). Innocuous, not noxious, input activates PKC γ interneurons of the spinal dorsal horn via myelinated afferent fibers. *J. Neurosci.* 28, 7936–7944. doi: 10.1523/JNEUROSCI.1259-08.2008
- Nicholls, J., and Saunders, N. (1996). Regeneration of immature mammalian spinal cord after injury. *Trends Neurosci.* 19, 229–234. doi: 10.1016/0166-2236(96)10021-7
- Norris, C. M., Blalock, E. M., Thibault, O., Brewer, L. D., Clodfelter, G. V., Porter, N. M., et al. (2006). Electrophysiological mechanisms of delayed excitotoxicity: positive feedback loop between nmda receptor current and depolarization-mediated glutamate release. *J. Neurophysiol.* 96, 2488–2500. doi: 10.1152/jn.00593.2005
- Pernas-Alonso, R., Schaffner, A. E., Perrone-Capano, C., Orlando, A., Morelli, F., Hansen, C. T., et al. (1996). Early upregulation of medium neurofilament gene expression in developing spinal cord of the wobbler mouse mutant. *Brain Res. Mol. Brain Res.* 38, 267–275. doi: 10.1016/0169-328x(95)00344-r
- Petitjean, H., Pawlowski, S. A., Fraine, S. L., Sharif, B., Hamad, D., Fatima, T., et al. (2015). Dorsal Horn Parvalbumin Neurons Are Gate-Keepers of Touch-Evoked Pain after Nerve Injury. *Cell. Rep.* 13, 1246–1257. doi: 10.1016/j.celrep.2015.09.080
- Petrova, V., Nieuwenhuis, B., Fawcett, J. W., and Eva, R. (2021). Axonal Organelles as Molecular Platforms for Axon Growth and Regeneration after Injury. *Int. J. Mol. Sci.* 22:1798. doi: 10.3390/ijms22041798
- Petrova, V., Pearson, C. S., Ching, J., Tribble, J. R., Solano, A. G., Yang, Y., et al. (2020). Protrudin functions from the endoplasmic reticulum to support axon regeneration in the adult CNS. *Nat. Commun.* 11, 5614. doi: 10.1038/s41467-020-19436-y
- Roppongi, R. T., Champagne-Jorgensen, K. P., and Siddiqui, T. J. (2017). Low-Density Primary Hippocampal Neuron Culture. *J. Vis. Exp.* 122:55000. doi: 10.3791/55000
- Russ, D. E., Cross, R. B. P., Li, L., Koch, S. C., Matson, K. J. E., Yadav, A., et al. (2021). A harmonized atlas of mouse spinal cord cell types and their spatial organization. *Nat. Commun.* 12:5722. doi: 10.1038/s41467-021-25125-1
- Schindelin, J., Arganda-Carreras, I., Frise, E., Kaynig, V., Longair, M., Pietzsch, T., et al. (2012). Fiji: an open-source platform for biological-image analysis. *Nat. Methods* 9, 676–682. doi: 10.1038/nmeth.2019
- Schwab, M. E., and Strittmatter, S. M. (2014). Nogo limits neural plasticity and recovery from injury. *Curr. Opin. Neurobiol.* 27, 53–60. doi: 10.1016/j.conb.2014.02.011

- Shen, Y., Tenney, A. P., Busch, S. A., Horn, K. P., Cuascat, F. X., Liu, K., et al. (2009). PTPsigma is a receptor for chondroitin sulfate proteoglycan, an inhibitor of neural regeneration. *Science* 326, 592–596. doi: 10.1126/science.1178310
- Song, M., Mohamad, O., Chen, D., and Yu, S. P. (2013). Coordinated Development of Voltage-Gated Na⁺ and K⁺ Currents Regulates Functional Maturation of Forebrain Neurons Derived from Human Induced Pluripotent Stem Cells. *Stem. Cells Dev.* 22, 1551–1563. doi: 10.1089/scd.2012.0556
- Spike, R. C., Puskar, Z., Andrew, D., and Todd, A. J. (2003). A quantitative and morphological study of projection neurons in lamina I of the rat lumbar spinal cord. *Eur. J. Neurosci.* 18, 2433–2448. doi: 10.1046/j.1460-9568.2003.02981.x
- Stahl, A. M., Ruthel, G., Torres-Melendez, E., Kenny, T. A., Panchal, R. G., and Bavari, S. (2007). Primary cultures of embryonic chicken neurons for sensitive cell-based assay of botulinum neurotoxin: implications for therapeutic discovery. *J. Biomol. Screen* 12, 370–377. doi: 10.1177/1087057106299163
- Sun, J., and Harrington, M. A. (2019). The Alteration of Intrinsic Excitability and Synaptic Transmission in Lumbar Spinal Motor Neurons and Interneurons of Severe Spinal Muscular Atrophy Mice. *Front. Cell. Neurosci.* 13:15. doi: 10.3389/fncel.2019.00015
- Sun, Z., Williams, D. J., Xu, B., and Gogos, J. A. (2018). Altered function and maturation of primary cortical neurons from a 22q11.2 deletion mouse model of schizophrenia. *Trans. Psychiat.* 8:85. doi: 10.1038/s41398-018-0132-8
- Takazawa, T., Croft, G. F., Amoroso, M. W., Studer, L., Wichterle, H., and MacDermott, A. B. (2012). Maturation of Spinal Motor Neurons Derived from Human Embryonic Stem Cells. *PLoS ONE* 7:e40154. doi: 10.1371/journal.pone.0040154
- Thomson, C. E., McCulloch, M., Sorenson, A., Barnett, S. C., Seed, B. V., Griffiths, I. R., et al. (2008). Myelinated, synapsing cultures of murine spinal cord – validation as an in vitro model of the central nervous system. *Eur. J. Neurosci.* 28, 1518–1535. doi: 10.1111/j.1460-9568.2008.06415.x
- Todd, A. J., Spike, R. C., and Polgár, E. (1998). A quantitative study of neurons which express neurokinin-1 or somatostatin sst2a receptor in rat spinal dorsal horn. *Neuroscience* 85, 459–473. doi: 10.1016/S0306-4522(97)00669-6
- Uyeda, A., and Muramatsu, R. (2020). Molecular Mechanisms of Central Nervous System Axonal Regeneration and Remyelination: A Review. *Int. J. Mol. Sci.* 21:8116. doi: 10.3390/ijms21218116
- van Niekerk, E. A., Tuszynski, M. H., Lu, P., and Dulin, J. N. (2016). Molecular and Cellular Mechanisms of Axonal Regeneration After Spinal Cord Injury. *Mol. Cell. Proteomics* 15, 394–408. doi: 10.1074/mcp.R115.053751
- Wilson, J. M., Hartley, R., Maxwell, D. J., Todd, A. J., Lieberam, I., Kaltschmidt, J. A., et al. (2005). Conditional Rhythmicity of Ventral Spinal Interneurons Defined by Expression of the Hb9 Homeodomain Protein. *J. Neurosci.* 25, 5710–5719. doi: 10.1523/JNEUROSCI.0274-05.2005
- Zeng, H., and Sanes, J. R. (2017). Neuronal cell-type classification: challenges, opportunities and the path forward. *Nat. Rev. Neurosci.* 18, 530–546. doi: 10.1038/nrn.2017.85
- Zhong, G., Díaz-Ríos, M., and Harris-Warrick, R. M. (2006). Intrinsic and Functional Differences among Commissural Interneurons during Fictive Locomotion and Serotonergic Modulation in the Neonatal Mouse. *J. Neurosci.* 26, 6509–6517. doi: 10.1523/JNEUROSCI.1410-06.2006

Conflict of Interest: The authors declare that the research was conducted in the absence of any commercial or financial relationships that could be construed as a potential conflict of interest.

Publisher's Note: All claims expressed in this article are solely those of the authors and do not necessarily represent those of their affiliated organizations, or those of the publisher, the editors and the reviewers. Any product that may be evaluated in this article, or claim that may be made by its manufacturer, is not guaranteed or endorsed by the publisher.

Copyright © 2022 Vargova, Kriska, Kwok, Fawcett and Jendelova. This is an open-access article distributed under the terms of the Creative Commons Attribution License (CC BY). The use, distribution or reproduction in other forums is permitted, provided the original author(s) and the copyright owner(s) are credited and that the original publication in this journal is cited, in accordance with accepted academic practice. No use, distribution or reproduction is permitted which does not comply with these terms.